Synthesis, characterization and antiproliferative activity of metal complexes with the Schiff base derived from the condensation 1 : 2 of 2,6-diformyl-4-methylphenol and 5,6-diamin...

ARTICLE *in* JOURNAL OF INORGANIC BIOCHEMISTRY · MAY 2008

Impact Factor: 3.44 · DOI: 10.1016/j.jinorgbio.2007.10.008 · Source: PubMed

5 AUTHORS, INCLUDING:

José Manuel Martínez-Martos
Universidad de Jaén
142 PUBLICATIONS **823** CITATIONS
SEE PROFILE

María Jesús Ramírez-Expósito
Universidad de Jaén
131 PUBLICATIONS **733** CITATIONS
SEE PROFILE

Available online at www.sciencedirect.com
ScienceDirect
Journal of Inorganic Biochemistry 102 (2008) 647–655
Journal of Inorganic Biochemistry
www.elsevier.com/locate/jinorgbio

Synthesis, characterization and antiproliferative activity of metal complexes with the Schiff base derived from the condensation 1:2 of 2,6-diformyl-4-methylphenol and 5,6-diamino-1,3-dimethyluracil

Nuria A. Illán-Cabeza [a], Francisco Hueso-Ureña [a], Miguel N. Moreno-Carretero [a,*], José M. Martínez-Martos [b], María J. Ramírez-Expósito [b]

[a] *Departamento de Química Inorgánica y Orgánica, Facultad de Ciencias Experimentales, Universidad de Jaén, Paraje Las Lagunillas s/n, 23071 Jaén, Spain*
[b] *Departamento de Ciencias de la Salud, Universidad de Jaén, 23071 Jaén, Spain*

Received 29 June 2007; received in revised form 13 October 2007; accepted 16 October 2007
Available online 24 October 2007

Abstract

A series of mononuclear complexes with Co(II), Ni(II), Cu(II), Zn(II), Hg(II), Mo(VI) and Pd(II) containing the ligand derived from the 1:2 condensation of 2,6-diformyl-4-methylphenol and 5,6-diamino-1,3-dimethyluracil (hereafter denoted as BDFDAAU) were synthesized. The complexes were characterized by elemental analysis, thermogravimetry (TG) and differential scanning calorimetry (DSC), IR, ^{1}H, ^{13}C and ^{15}N NMR, UV–visible–near IR (UV–VIS–NIR), EPR and magnetic measurements. The deprotonated ligand in the phenolic oxygen shows a symmetric tridentate coordination mode through the two azomethine nitrogen atoms and the phenolic oxygen atom whereas the coordination of the neutral ligand takes place through the phenolic oxygen atom and one azomethine nitrogen atom. In the Mo(VI) complex, the ligand is bideprotonated in the phenolic oxygen and an amino group from one uracil unit; so, the coordination mode changes again into an asymmetric way: phenolic oxygen atom, one azomethine nitrogen atom and the nitrogen atom from the deprotonated amino group. The antiproliferative behaviour against the five human tumor cell lines (human neuroblastoma NB69, human breast cancer MCF-7 and EVSA-T, human glioma H4 and human bladder carcinoma cell line ECV) suggested a modulator behaviour, according to the concentration, of cell growth due to their estrogen-like characteristics.

Keywords: 2,6-diformyl-4-methylphenol; Schiff bases complexes; Uracil; Antiproliferative activity

1. Introduction

The chemistry of phenoxo compounds has a great interest in the design of compartmental ligands to study the interaction in polynuclear metal complexes. Planar ligands with amine or imine donor groups and bridging phenolic oxygens are referred to as Robson-type ligands [1]. The compartmental ligands contain two adjacent, similar to dissimilar compartments which can coordinate two identical or different metal ions in close proximity. The donor groups of these ligands provides a significant diversification of the coordination sites making them good candidates for metal ion complexation and for mimicking biological systems. The study of their stereochemical, electronic, magnetic, catalytic and spectroscopic properties have allowed the proposal of probes for some important applications [2–16]. Increasing attention, especially in bioinorganic chemistry for modelling the activity centre of metalloenzymes and metalloproteins and in the search for appropriate systems for activating simple molecules, has occurred. Also, it has been studied the biological activity of related compounds with interesting results [17–19].

* Corresponding author. Tel.: +34 953 212738; fax: +34 953 211876.
E-mail address: mmoreno@ujaen.es (M.N. Moreno-Carretero).

0162-0134/$ - see front matter © 2007 Elsevier Inc. All rights reserved.
doi:10.1016/j.jinorgbio.2007.10.008

The Robson-type ligands are usually obtained by condensation of appropriate formyl and amine precursors. In our case, we have used a uracil derivative, giving as a result a compartmental "end-off" type ligand. It is well known that uracil derivatives play an important role in many biological systems for their chemotherapeutic effects. Due to the biological significance of uracil, we have studied the potential activity of the ligand and its metal complexes against some tumoral cell lines. The aim of the present study was to examine the effect on cell proliferation although at low doses might show estrogenic activity which makes them acting like modulators of the cell growth.

In the present paper we report on the synthesis, characterization and biological properties of novel mononuclear complexes with a ligand derived from the 1:2 condensation of 2,6-diformyl-4-methylphenol and 5,6-diamino-1,3-dimethyluracil.

2. Experimental

2.1. Apparatus

C, H, N and S microanalyses were performed on a Fisons EA1108 apparatus. The loss of water was determined from the thermogravimetry (TG) and differential scanning calorimetry (DSC) plots (Mettler TA-3000 system). Conductivity measurements have been carried out using 10^{-3} M freshly prepared dimethylformamide (DMF) solutions on a Hanna HI8820 instrument. IR spectra were measured on Perkin–Elmer FT-IR 1760-X (KBr pellets, 4000–400 cm^{-1}) and FT-IR Bruker Vector-22 spectrophotometer (polyethylene pellets, 600–220 cm^{-1}). ^{15}N, ^{13}C and ^{1}H NMR spectra were recorded using a Bruker AM-300 apparatus (DMSO-d_6 solutions). Electronic spectra (diffuse reflectance, 240–1500 nm) were recorded on a Perkin–Elmer UV/VIS/NIR Lambda-19 machine using a $BaSO_4$ pellet as reference. Electron paramagnetic resonance (EPR) spectra were obtained in the X-band at room temperature on a Bruker ESP 300E spectrometer, with a microwave frequency of 9.79 GHz and a modulation frequency of 100 kHz. Magnetic susceptibility measurements were carried out at room temperature on a Sherwood Scientific magnetic balance and on a Manics DSM-8 system (70–290 K).

2.2. Synthetic procedures

Commercial grade chemicals were used without further purification. In all cases, analytical (C, H, N, S) and thermogravimetric data (H_2O) for the isolated compounds fit well with the reported formulas. The Schiff base BDFDAAU [(4,4′-[(2-hydroxy-5-methyl-1,3-phenylene)diethene-2,1-diyl]-bis-(5-amino-2,6-dimethylcyclohex-4-ene-1,3-dione, see Fig. 1] was prepared by reacting 2,6-diformyl-4-methylphenol and 5,6-diamino-1,3-dimethyluracil in a 1:2 ratio in MeOH medium (ca. 40 mL) containing a few drops of glacial AcOH, after refluxing the resulting solution for several hours. The yellow compound was filtered off, washed with EtOH and Et_2O and air dried (yield ca. 90%). BDFDAAU·3/2H_2O ($C_{21}H_{27}N_8O_{6.5}$). Characterizational data were as follows: NMR assignments were made from ^{1}H, ^{13}C, DEPT (distortionless enhancement by polarization transfer), ^{13}C–^{1}H HMQC (heteronuclear multiple-quantum coherence), ^{13}C–^{1}H HMBC (heteronuclear multiple bond correlation) and ^{15}N–^{1}H HMBC spectra (δ, ppm). ^{1}H NMR: 3.39 (N1B–CH_3, N1C–CH_3), 3.16 (N3B–CH_3, N3C–CH_3), 2.30 (C4ACH_3), 9.84 (H21A, H61A), 7.61 (H3A, H5A), 7.18 (H6B, H6C), 12.93 (OH); ^{13}C NMR: 30.41 (C1B, C1C), 149.73 (C2B, C2C), 27.34 (C3B, C3C), 157.20 (C4B, C4C), 99.23 (C5B, C5C), 152.50 (C6B, C6C), 151.36 (C21A, C61A), 156.14 (C1A), 123.09 (C2A, C6A), 130.26 (C3A, C5A), 127.53 (C4A), 20.18 (C41A); ^{15}N NMR: 1.36 (N1B, N1C), 34.84 (N3B, N3C), 175.06 (N21A, N61A), –37.78 (N6B, N6C).

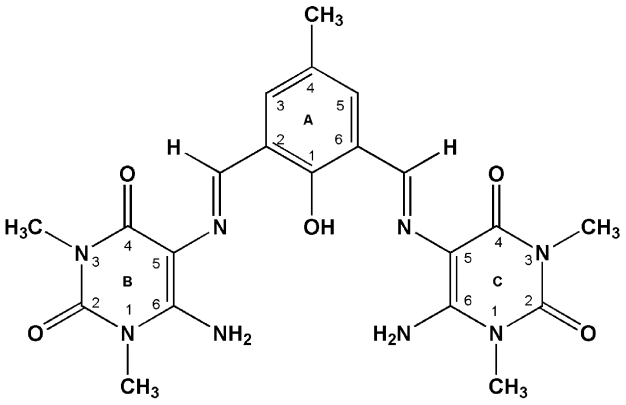

Fig. 1. Structure and nomenclature of the ligand BDFDAAU.

2.3. Preparation of the complexes

2.3.1. $CoCl_2$(BDFDAAU)·3/2H_2O, MoO_2(BDFDAAUH_{-2})·3H_2O and $PdCl_2$(BDFDAAU)·1/2H_2O

The synthesis of these compounds was carried out by reacting 0.25 mmol of the ligand with 0.25 mmol of $CoCl_2·6H_2O$, 0.036 mmol of $(NH_4)_6Mo_7O_{24}$ and 0.25 mmol of K_2PdCl_4 in 30 mL MeOH. A suspension of the reaction product was obtained which was heated at 60 °C and stirred for about four hours and left to cool at room temperature before getting filtered off. The solids were washed with EtOH and Et_2O and air dried. $CoCl_2$(BDFDAAU)·3/2H_2O ($CoC_{21}H_{27}N_8O_{6.5}Cl_2$, yield ca. 66%, brown): $\Lambda_M = 53$ mho cm^2 mol^{-1}. MoO_2(BDFDAAUH$_{-2}$)·3H_2O ($MoC_{21}H_{28}N_8O_{10}$, yield ca. 65%, red): $\Lambda_M = 7$ mho cm^2 mol^{-1}; ^{1}H NMR: 3.49(N1B–CH_3, N1C–CH_3), 3.12 (N3B–CH_3, N3C–CH_3), 2.29 (C4ACH_3), 9.97, 10.09 (H21A, H61A), 7.64 (H3A, H5A), 7.34 (−NH_2), 8.19 (−N–H). $PdCl_2$(BDFDAAU)·1/2H_2O ($PdC_{21}H_{25}N_8O_{5.5}Cl_2$, yield ca. 75%, red): $\Lambda_M =$ 49 mho cm^2 mol^{-1}.

2.3.2. Ni(SCN)(BDFDAAUH$_{-1}$) and Cu(SCN)(BDFDAAUH$_{-1}$)

The ligand (0.25 mmol) and 0.25 mmol of KSCN were suspended in hot MeOH (40 mL). After that, 0.25 mmol of corresponding metallic chloride was added, the precipitation of a powdered solid taking place. The solids were washed with EtOH and Et_2O and air dried. Ni(SCN)(BDFDAAUH$_{-1}$) ($NiC_{22}H_{23}N_9O_5S$, yield ca. 80%, red): $\Lambda_M = 34$ mho cm^2 mol^{-1}. Cu(SCN)(BDFDAAUH$_{-1}$) ($CuC_{22}H_{23}N_9O_5S$, yield ca. 83%, brown): $\Lambda_M = 79$ mho cm^2 mol^{-1}.

2.3.3. Ni(ClO$_4$)(BDFDAAUH$_{-1}$)·2H$_2$O, Cu(ClO$_4$)(BDFDAAUH$_{-1}$), Zn(ClO$_4$)(BDFDAAUH$_{-1}$)·3/2H$_2$O and Hg(ClO$_4$)$_2$(BDFDAAU)

A suspension of BDFDAAU (0.25 mmol) in EtOH (50 mL), MeOH (50 mL), MeOH/MeCN (1:1) (50 mL) and EtOH/MeCN (1:1) (40 mL), respectively, was mixed with the corresponding perchlorate salt. The resulting solutions were heated at 60 °C for three hours. After standing at room temperature for several days, the solutions gave different solids which were filtered off and washed with EtOH and Et_2O. Ni(ClO$_4$)(BDFDAAUH$_{-1}$)·2H$_2$O ($NiC_{21}H_{27}N_8O_{11}Cl$, yield ca. 62%, red): $\Lambda_M = 84$ mho cm^2 mol^{-1}. Cu(ClO$_4$)(BDFDAAUH$_{-1}$) ($CuC_{21}H_{23}N_8O_9Cl$, yield ca. 58%, brown): $\Lambda_M = 44$ mho cm^2 mol^{-1}. Zn(ClO$_4$)(BDFDAAUH$_{-1}$)·3/2H$_2$O ($ZnC_{21}H_{27}N_8O_{10.5}Cl$, yield ca. 48%, red): $\Lambda_M = 87$ mho cm^2 mol^{-1}; ^{1}H NMR: 3.37 (N1B–CH_3, N1C–CH_3), 3.15 (N3B–CH_3, N3C–CH_3), 2.28 (C4ACH_3), 9.66 (H21A, H61A), 7.61 (H3A, H5A), 7.25 (H6B, H6C); ^{13}C NMR: 30.40 (C1B, C1C), 149.63 (C2B, C2C), 27.40 (C3B, C3C), 157.18 (C4B, C4C), 97.80 (C5B, C5C), 151.99 (C6B, C6C), 150.50 (C21A, C61A), 153.58 (C1A), 121.90 (C2A, C6A), 132.40 (C3A, C5A), 127.00 (C4A), 20.10 (C41A); ^{15}N NMR: 115.22 (N1B, N1C), 142.13 (N3B, N3C), 269.36 (N21A, N61A), 73.63 (N6B, N6C). Hg(ClO$_4$)$_2$(BDFDAAU) ($HgC_{21}H_{24}N_8O_{13}Cl_2$, yield ca. 61%, brown): $\Lambda_M = 53$ mho cm^2 mol^{-1}.

2.3.4. Cu(NO$_3$)(BDFDAAUH$_{-1}$)·2H$_2$O

A solution of 0.5 mmol of Cu(NO$_3$)·6H$_2$O was added to a stirred suspension of BDFDAAU in 25 mL MeOH, obtaining a green solid which was filtered off, washed with EtOH and Et_2O and air dried. Cu(NO$_3$)(BDFDAAUH$_{-1}$)·2H$_2$O ($CuC_{21}H_{27}N_9O_{10}$, yield ca. 78%, green): $\Lambda_M = 68$ mho cm^2 mol^{-1}.

2.3.5. ZnCl(BDFDAAUH$_{-1}$)·5/2H$_2$O

An orange suspension was formed after the reaction of 0.5 mmol of $ZnCl_2$ with 0.25 mmol of BDFDAAU in 30 mL MeCN. The resulting solid was filtered off, washed with EtOH and Et_2O and air dried. ZnCl(BDFDAAUH$_{-1}$)·5/2H$_2$O ($ZnC_{21}H_{28}N_8O_{7.5}Cl$, yield ca. 73%, red): $\Lambda_M = 15$ mho cm^2 mol^{-1}.

Caution: Perchlorate salts are potentially explosive and must be handled with care.

2.4. Biological assays

Five human tumour cell lines (human breast cancer MCF-7 (hormone-dependent) and EVSA-T (hormone-independent) cell lines, human neuroblastoma NB69, human glioma H4 and human bladder carcinoma cell line ECV) have been studied in this work. Cell lines were grown in 5% fetal bovine serum (FBS)-supplemented Dubelcco's modified Eagle's medium (DMEM) with penicillin (100 units/mL) and streptomycin (0.1 mg/mL). Cells were incubated at 37 °C in a modified atmosphere of 5% CO_2/95% air. Freedom from mycoplasma contamination was checked regularly by testing with Hoechst 33528.

To set up the colorimetric cytotoxic assay (CCA) cells were trypsinized from monolayer and diluted to 4×10^4 cells/mL. Cells were in exponential phase of growth during the whole experiment. Aliquots of 1 mL of cells were pipetted into wells of 24-well tissue culture plates (Nunc) and the plates were incubated for 24 h. The different complexes, the ligand (BDFDAAU) and the metallic salts, were then added to the wells in a volume of 1 mL per well at a range of concentrations (2, 4, 6, 8, and 10 μM), each dose being used in at least four replicate wells. After 3 days incubation, the mediums were removed and the cultures, were washed with PBS prior to fixation with 10% trichloroacetic acid (TCA) (4 °C) for 30 min and then washed with tap water to remove TCA. Plates were air dried and then stored until use. TCA-fixed cells were stained for 20 min with 0.4% (w/v) sulforhodamine B (SRB) (Sigma) dissolved in 1% acetic acid. At the end of staining period, SRB was removed and cultures were rinsed with 1% acetic acid to remove unbound dye. The cultures were air dried and bound dye was solubilised with 10 mM Tris base (pH 10.5). Optical density (OD) was read in ThermoLabsystems multiscan Ascent plate reader at 492 nm. The photometer response was linear with dye concentration and it was proportional to cell numbers counted in parallel with a hemocytometer.

3. Results and discussion

The presence of water has been corroborated from the TG and DSC studies. The pyrolitic degradation in the TG plots begins around 50 °C until 200 °C. The $CoCl_2$(BDFDAAU)·2H$_2$O and ZnCl(BDFDAAUH$_{-1}$)·5/2H$_2$O complexes have two endothermic peaks, appearing the second one over 140–160 °C which may correspond to one coordinated water molecule. The Ni(ClO$_4$)(BDFDAAUH$_{-1}$)·2H$_2$O and Zn(ClO$_4$)(BDFDAAUH$_{-1}$)·3/2H$_2$O seem to have two and one coordinated water molecules, respectively. The loss of water molecules for the rest of the complexes takes place at lower temperatures, thus suggesting no coordination.

The molar conductivity values were measured in DMF solutions except Ni(SCN)(BDFDAAUH$_{-1}$) and $PdCl_2$-(BDFDAAU)·1/2H_2O compounds whose molar conductivities were measured in DMSO because their low solubility.

All the complexes with the deprotonated ligand show a non-electrolyte nature except $Zn(ClO_4)$(BDFDAAUH$_{-1}$)·3/2H_2O and $Ni(ClO_4)$(BDFDAAUH$_{-1}$)·2H_2O. The Cu(SCN)(BDFDAAUH$_{-1}$) compound seems to be 1:1 electrolyte, but the IR spectrum shows that thiocyanate group is coordinated to the metal through the nitrogen atom, so the high conductivity value can be due to solvolysis processes. The complexes with the ligand in its neutral form behave as non-electrolytes. The Mo(VI) complex with the bideprotonated ligand presents a non-electrolyte character [20].

To test the different BDFDAAU coordination possibilities, theoretical calculations were carried out by means of the semiempirical method PM3–RHF as implemented in the HYPERCHEM 6.0 program package [21]. The molecular structures were generated with the molecular builder inside HYPERCHEM and optimised following the Polak–Ribiere algorithm until the root mean square gradient reached 0.1 kcal $Å^{-1}$ mol^{-1}. Coordination possibilities were analyzed from the contribution of the AOs of potential donor atoms to the occupied σMOs higher in energy and, so, more available for establish M–L bonds. The studies were applied to the ligand in the neutral form and deprotonated in the phenolic oxygen atom. The results of the coordinating capability of the neutral form were very confuse and it is very conditioned for the formation of an intramolecular H-bond and the originated steric hindrance. The deprotonated ligand clearly showed three potential donor positions: O_{ph} and two N_{az}.

Infrared spectral data of BDFDAAU and its metal complexes are listed in Table 1. By comparing with those reported for several similar compounds, a number of bands were tentatively assigned [22,23].

The IR spectra show a band over 3400–3300 cm^{-1} range assignable to ν(N–H) vibration which may be broadened by the presence of lattice water molecules or by the establishment of an intramolecular H-bond in complexes with the ligand in its neutral form [25,26]. The comparison of IR spectra of the complexes with the one corresponded to the ligand BDFDAAU shows a displacement of the ν(C=N) and ν(C–O_{ph}) vibration modes. The ν(C=N) stretching vibration is normally displaced to upper wavenumber (ca. 3–34 cm^{-1}) because of the bond stabilization on the azomethine moiety after the coordination. Complexes with deprotonated and neutral BDFDAAU ligand show a small shift in the ν(C–O_{ph}) mode (ca. 3–26 cm^{-1}) as consequence of two effects: (a) The shift of C–O stretching vibration of phenolate group to higher frequencies after the loss of the proton and (b) The lower wavenumber displacement promoted by the coordination [22,23]. In the far-infrared region, bands associated to the M–N_{az} and M–O_{ph} have been assigned [26,27] in accordance with data found in the literature.

Table 1
Selected IR data (in cm^{-1}) for metal-free and metal (Co, Ni, Cu, Zn, Mo, Pd and Hg) complexes of BDFDAAU[a]

Compound	ν(N–H)	ν(C=O)	ν(C=N) + ν(C=C)	ν(C–O)	ν(M–$O_{ph.}$)	ν(M–$N_{azo.}$)	ν(M–Cl)
BDFDAAU	3398s	1690s	1554m	1223m	–	–	–
		1626m	1516m				
$CoCl_2$(BDFDAAU)·3/2H_2O	3410s	1704vs	1573m	1220m	420w	312w	326w
		1651m	1516m				
$Ni(ClO_4)$(BDFDAAUH$_{-1}$)·2H_2O	3420s	1694s	1588m	1232m	420w	316w	–
		1621m	1519m				
Ni(SCN)(BDFDAAUH$_{-1}$)	3399s	1705s	1524m	1227m	431w	327w	–
		1660m				337w	
Cu(SCN)(BDFDAAUH$_{-1}$)	3409s	1704s	1537m	1226m	418w	327w	–
		1660m	1510m				
						341w	
$Cu(ClO_4)$(BDFDAAUH$_{-1}$)	3415s	1691s	1560m	1245m	411w	317w	–
		1636m	1515m				
$Cu(NO_3)$(BDFDAAUH$_{-1}$)·2H_2O	3413s	1700s	1551m	1226m	406w	307w	–
		1659m	1501m			318w	
$Zn(ClO_4)$(BDFDAAUH$_{-1}$)·3/2H_2O	3416s	1694s	1581m	1249m	419w	339w	–
		1636m	1520m				
ZnCl(BDFDAAUH$_{-1}$)·5/2H_2O	3327s	1692s	1578m	1233m	419w	347w	298w
		1654m	1516m				
MoO_2(BDFDAAUH$_{-2}$)·3H_2O	3415vs	1680s	1553m	1225m	425w	311w	–
	3319vs	1632m	1505m			330w	
$PdCl_2$(BDFDAAU)·1/2H_2O	3469s	1698s	1568m	1231m	410w	307w	266w
		1637m	1520m				274w
$Hg(ClO_4)_2$(BDFDAAU)	3417s	1696s	1581m	1224m	409w	329w	–
		1636m	1520m				

[a] s, strong; m, medium; w, weak.

Table 2
Electronic spectra, EPR and magnetic measurements for Co, Ni and Cu complexes of BDFDAAU

Compounds	Electronic spectra		EPR		μ[a]
	ν (cm^{-1})	Transition	$g_{\parallel}$	$g_{\perp}$	
$CoCl_2(BDFDAAU)\cdot 3/2H_2O$	8500	$^4E'' \leftarrow {}^4A_2'$			4.8
	14100	$^4E' \leftarrow {}^4A_2'$			
	15300	$^4A'(P) \leftarrow {}^4A_2'$			
	19600	$^4E''(P) \leftarrow {}^4A_2'$			
		$O_{ph}^- \rightarrow$ Co LMCT			
	23100	$Cl \rightarrow$ Co LMCT			
$Ni(ClO_4)(BDFDAAUH_{-1})\cdot 2H_2O$	9700	$^3T_{2g} \leftarrow {}^3A_{2g}$			2.7
	11400	$^3T_{1g} \leftarrow {}^3A_{2g}$			
	18400	$^3T_{1g}(P) \leftarrow {}^3A_{2g}$			
	20900	$O_{ph}^- \rightarrow$ Ni LMCT			
$Ni(SCN)(BDFDAAUH_{-1})$	17900	*d–d*			0.6
	19700	$O_{ph}^- \rightarrow$ Ni LMCT			
	21800	$SCN \rightarrow$ Ni LMCT			
$Cu(SCN)(BDFDAAUH_{-1})$	11700	*d–d*	2.29	2.04	1.9
	15300	*d–d*			
	20000	$O_{ph}^- \rightarrow$ Cu LMCT			
	23100	$SCN \rightarrow$ Cu LMCT			
$Cu(ClO_4)(BDFDAAUH_{-1})$[b]	16100	*d–d*	2.15	2.00	1.5
	20000	$O_{ph}^- \rightarrow$ Cu LMCT			
$Cu(NO_3)(BDFDAAUH_{-1})\cdot 2H_2O$[b]	15200	*d–d*	2.21	2.05	1.5
	20500	$O_{ph}^- \rightarrow$ Cu LMCT			

[a] Corrected by diamagnetism. Calculated at room temperature.
[b] Observed EPR hyperfine interaction.

Over 1700–1650 cm^{-1} two absorptions are observed which may be assigned to the stretching vibrations of both carbonyl groups; the first, due to ν(C2═O), at upper wavenumber, and the second, due to ν(C4═O), which may be overlapped with ν(C═N) and ν(C═C). The complexes show a displacement to lower wavenumbers of ν(C4═O) as a consequence of the electronic redistribution upon coordination.

The Mo(VI) compound shows two sharp intense bands around 900 cm^{-1} assigned to the *cis* MoO_2^{2+} group [26]. Also, in the 3400−3300 cm^{-1} range two sharp bands are observed as consequence of 6-amino group deprotonation from one uracil ring. As it has been previously reported, nitrogen atom from the 6-amino group acts as metal binding site if it is deprotonated [24]. So, the ligand behaves as a tridentate ligand through the oxygen phenolic atom, one azomethine nitrogen and the nitrogen atom from the amino group deprotonated.

In conclusion, if the 6-amino group does not act as a donor group and the phenolic group is deprotonated, the ligand coordination may be produced through O_{ph} atom and the N_{az} atoms but if the ligand acts in neutral form, one imine nitrogen might be involved in an intramolecular H-bond with the phenolic group, so the coordination of the ligand could take place in a bidentate mode.

The perchlorate vibrations are observed in the 1190–1080 cm^{-1} range, showing in all cases three bands which suggest a monodentate behaviour [26]. The molar conductivity studies indicate some complexes with uncoordinated perchlorate groups, so the loss of symmetry T_d to C_{3v} could be due to H-bond formation or to a weak coordination of the perchlorate group to the metal ion. A strong sharp band at 1385 cm^{-1} for $Cu(NO_3)(BDFDAAUH_{-1})\cdot 2H_2O$ complex has been assigned to the ν(N–O) vibration of a free nitrate group [26]. The complexes Ni(SCN)-(BDFDAAUH$_{-1}$) and Cu(SCN)(BDFDAAUH$_{-1}$) show a very intense band at 2119 and 2106 cm^{-1}, respectively, which corresponds to ν(CN) stretching vibration. At lower frequency, δ(SCN) band around 500 cm^{-1} also appears. The frequency range in which the two absorptions appear, strongly suggests the presence of an N-coordinated thiocyanate group [26]. The halocomplexes exhibit one or two bands of weak-medium intensity in 250–330 cm^{-1} range attributable to M–X stretching mode. The MX vibrations are very useful in determining the stereochemistry of the complex and in our case, the presence of two ν(M–X) bands in palladium(II) compound seems to indicate two halide atoms in a *cis* arrangement [26,27].

In the present work, the ^1H, ^{13}C and ^{15}N NMR chemical shifts for complexes $Zn(ClO_4)(BDFDAAUH_{-1})\cdot 3/2H_2O$ and $MoO_2(BDFDAAUH_{-2})\cdot 3H_2O$ are included. The coordination mode of the deprotonated ligand in the complexes deduced by means of the IR spectral data is confirmed by general deshielding of some signals in NMR. It has not been possible to record the NMR spectra of Pd(II), Hg(II) and the low-spin diamagnetic Ni(II) compounds due to their low solubility in DMSO-d_6. The NMR spectra of the other compounds display signals at the same values of chemical shift than the free ligand, clearly indicating that these compounds may undergo strong solvolysis.

On comparing the ^1H NMR spectra of $Zn(ClO_4)$-(BDFDAAUH$_{-1}$)$\cdot 3/2H_2O$ with the one of the free ligand,

the disappearance of the phenolic proton signal due to deprotonation and the upfield shift of both azomethine protons (0.18 ppm) can be observed. The Mo(VI) complex shows two signals for azomethine protons and for the 6-amino group (one for deprotonated amino and one for the neutral amino group), one of them being deshielded with respect to the other which appears at similar chemical shift than in the spectrum of free ligand. These downfield shifts can be explained for the intense electrondrawing effect which presents Mo(VI) ion in the MoO_2^{2+} moiety and also for the possible asymmetric coordination pattern (O_{ph}, N_{az}, N_{im}) due to the dianionic $BDFDAAUH_{-2}$ ligand.

The comparison of the ^{13}C NMR spectrum of Zn(II) compound and the ligand leads to a similar conclusion. The carbon linked to the phenolic oxygen atom is upfield shifted (2.56 ppm) which suggests the involvement in the coordination of this oxygen atom. The signals assigned to the C5B–C5C and C2A–C6A are also deshielded because of their proximity to the donor atoms involved in the coordination process.

The large differences in the ^{15}N chemical shifts observed for Zn(II) compound (~100 ppm) indicate changes in the charge redistribution induced by the complexation.

The electronic and EPR spectral data for the complexes are summarized in Table 2. They show similar features containing strong absorptions bands with maxima between 42,000 and 28,000 cm^{-1}, which may be assigned to intraligand transitions. These bands have a shoulder around 20,000 cm^{-1} assigned to a O^-(phenolate) → M charge transfer [9]. The molybdenum(VI) complex shows a band at 20,700 cm^{-1} assignable to a π → π transition (O → Mo).

The spectrum of $CoCl_2(BDFDAAU)\cdot 3/2H_2O$ exhibits four *d–d* bands at 8500, 14100, 15300 and 19600 cm^{-1} that are attributed to a bipyramidal trigonal model [28]; the last one may include the $O_{ph}^- \rightarrow Co$ ligand-to-metal charge transfer band. Also, a $Cl \rightarrow Co$ LMCT band at 23,100 cm^{-1} is observed. The effective magnetic moment at room temperature is coherent with this geometry.

The complex $Ni(ClO_4)(BDFDAAUH_{-1})\cdot 3/2H_2O$ presents three bands at 9700, 11400 and 18400 cm^{-1} which can be assigned to a Ni(II) in an octahedral environment. The effective magnetic moment value is in accordance with the spin only magnetic moment value [29]. The spectrum of $Ni(SCN)(BDFDAAUH_{-1})$ exhibits one *d–d* band at 17900 cm^{-1} which is indicative of a square planar geometry because the eight electrons of Ni(II) are paired in the four low-lying *d* orbitals and these orbitals are often so close together in energy that individual transitions there from to the upper *d* level, cannot be distinguished [28]. There is an absorption band around 22,000 cm^{-1} assignable to a SCN → Ni(II) ligand-to-metal charge transfer. This compound is diamagnetic, although when diamagnetic corrections were done, $\mu_{eff} = 0.6$ BM was found, which is in accordance with a square-planar structure [29].

All the copper(II) complexes show a *d–d* transition in the 15,000–17,000 cm^{-1} range which is typical of Cu(II) complexes with tetragonal symmetry. The band maxima of the copper(II) complexes reported in this work were deconvoluted into Gaussian component bands in the visible region. Starting from a set of six peaks, computer iteration processes for experimental curves fitting were carried out until a minimum value to minimize the standard deviation from the calculated ones, reaching a standard deviation of 0.004 absorbance units. Thus, two peaks for the three copper spectra were obtained ($Cu(ClO_4)$-$(BDFDAAUH_{-1})$: 15000, 18600 cm^{-1}; $Cu(NO_3)(BDFDAAUH_{-1})\cdot 2H_2O$: 11100, 15800 cm^{-1}; $Cu(SCN)$-$(BDFDAAUH_{-1})$: 12000, 15800 cm^{-1}). These bands are assignable to the transitions from the ^2A and ^2B terms in which the fundamental ^2E term is splitted as consequence of Jahn–Teller effect [30] to the non-splitted ^2T term. The no splitting of the ^2T term could be explained assuming the distortion of the geometry is not enough to the energy differences between d_{xy}, d_{xz} and d_{yz} orbitals cannot be observed. The magnetic moment values at room temperature are in the expected range for the spin only contribution, the compounds being magnetically diluted monomeric units [31]. The magnetic susceptibility measurements for $Cu(NO_3)(BDFDAAUH_{-1})\cdot 2H_2O$ has been successfully fitted to the Curie–Weiss law ($\chi_M = C/(T-\theta)$, $C = 0.091$ cgsu K mol^{-1}, $\theta = 23$ K, $r = 0.9984$). The θ value suggests the existence of antiferromagnetic interactions [31]. The EPR powder spectra at room temperature are axial with a $2 < g_\perp < g_\parallel$ sequence, which indicates Cu(II) centers in a d_{x2-y2} ground state [32].

4. Biological studies

In this work we have studied the potential activity of the ligand and its metal complexes against some tumoral cell lines. The reported preliminary studies are focused in knowing the proliferative or antiproliferative behaviour

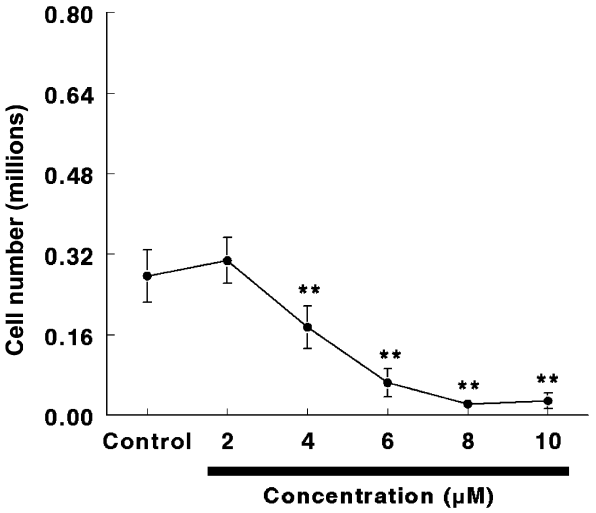

Fig. 2. Growth inhibition curves (results expressed as mean ± SD; $n = 4$; $^{**}p < 0.001$) for human glioma NB69 measured by the colorimetric cytotoxicity assay (CCA) after the treatment with BDFDAAU.

of the tested compounds and further studies should be necessary to allow a deeper understanding of the mechanism involved in these processes.

The treatment of the different complexes showed similar effects in all the tumoral cell lines used. For this reason, we only show the growth curves for human neuroblastoma NB69 measured by the CCA after the treatment of the ligand and the different complexes (Fig. 2). As it was previously reported [33], the solvent (dimethylsulfoxide, DMSO) shows no effect in cell growth.

The Ni(II) complexes showed an antiproliferative behaviour for the range of concentration studied (Fig. 3). At concentrations of 6 μM, cell growth decreased significantly. The same discussion may be done for the complexes $Cu(SCN)(BDFDAAUH_{-1})$, $Cu(ClO_4)(BDFDAAUH_{-1})$ (Fig. 4), $CoCl_2(BDFDAAU)\cdot 3/2H_2O$ and $Hg(ClO_4)_2$-(BDFDAAU) (Fig. 6); so, it is suggested that complexation of BDFDAAU with these metals has a synergic effect on the antiproliferative activity perhaps with a apoptotic behaviour although further studies are needed to clarify this topic.

The complexes $Cu(NO_3)(BDFDAAUH_{-1})$ (Fig. 4), $MoO_2(BDFDAAUH_{-2})$ and $PdCl_2(BDFDAAU)\cdot 1/2H_2O$ (Fig. 6) stimulated cell proliferation at low concentrations. This fact has been extensively described for heavy metals such as cadmium, which binds to and activates responses mediated by estrogen receptors (ER), thus behaving as a new class of nonsteroidal environmental estrogens [34–36]. However, higher concentrations (4–10 μM) decreased significantly cell growth suggesting a non-specific effect of

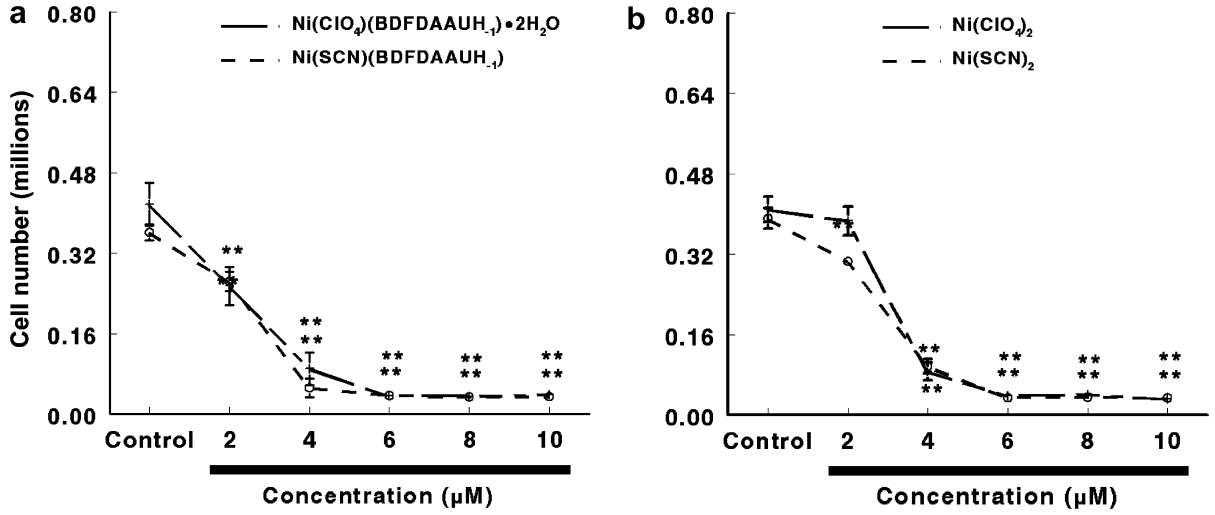

Fig. 3. Growth inhibition curves (results expressed as mean ± SD; $n = 4$; $^{**}p < 0.001$) for human glioma NB69 measured by the colorimetric cytotoxicity assay (CCA) after the treatment with (a) $Ni(ClO_4)(BDFDAAUH_{-1})\cdot 2H_2O$ and $Ni(SCN)(BDFDAAUH_{-1})$ and (b) $Ni(ClO_4)_2$ and $Ni(SCN)_2$.

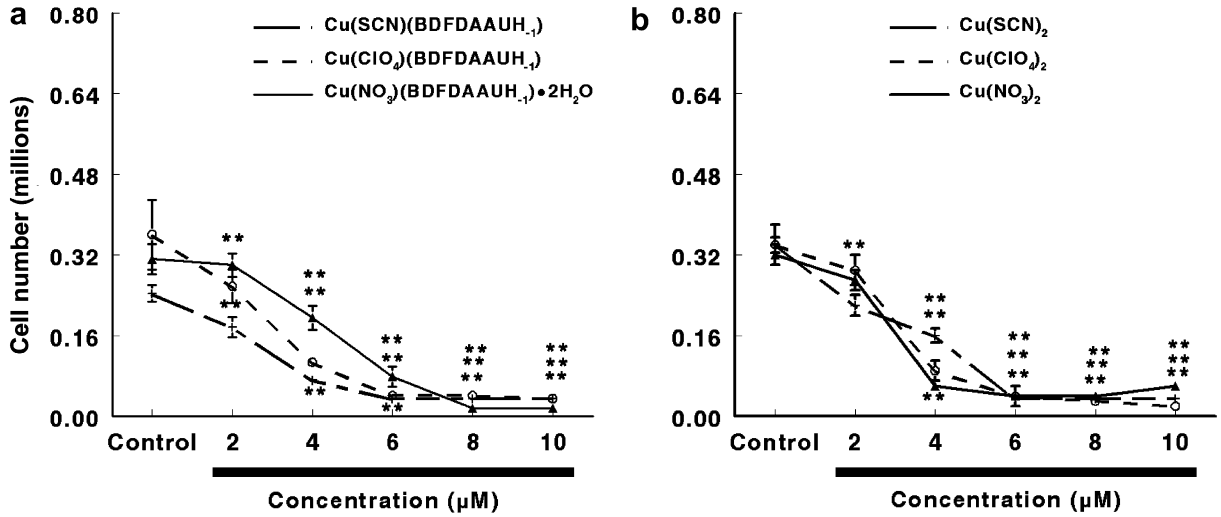

Fig. 4. Growth inhibition curves (results expressed as mean ± SD; $n = 4$; $^{**}p < 0.001$) for human glioma NB69 measured by the colorimetric cytotoxicity assay (CCA) after the treatment with (a) $Cu(ClO_4)(BDFDAAUH_{-1})$, $Cu(SCN)(BDFDAAUH_{-1})$ and $Cu(NO_3)(BDFDAAUH_{-1})\cdot 2H_2O$ and (b) $Cu(ClO_4)_2$, $Cu(SCN)_2$ and $Cu(NO_3)_2$.

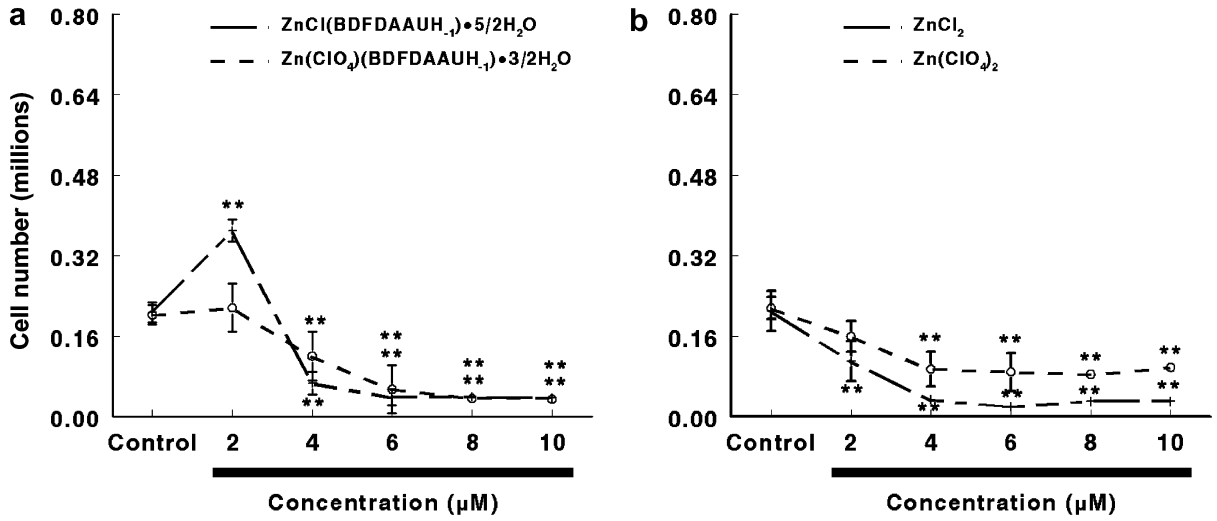

Fig. 5. Growth inhibition curves (results expressed as mean ± SD; $n = 4$; $^{**}p < 0.001$) for human glioma NB69 measured by the colorimetric cytotoxicity assay (CCA) after the treatment with (a) $Zn(ClO_4)(BDFDAAUH_{-1})\cdot 3/2H_2O$ and $ZnCl(BDFDAAUH_{-1})\cdot 5/2H_2O$ and (b) $Zn(ClO_4)_2$ and $ZnCl_2$.

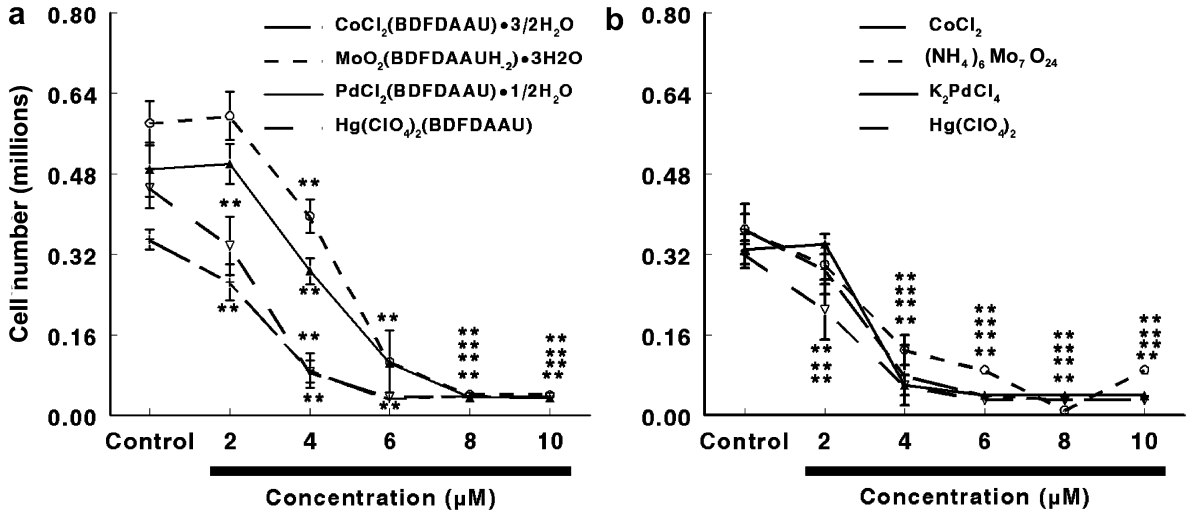

Fig. 6. Growth inhibition curves (results expressed as mean ± SD; $n = 4$; $^{**}p < 0.001$) for human glioma NB69 measured by the colorimetric cytotoxicity assay (CCA) after the treatment with (a) $CoCl_2(BDFDAAU)\cdot 3/2H_2O$, $MoO_2(BDFDAAUH_{-2})\cdot 3H_2O$, $PdCl_2(BDFDAAU)$, and $Hg(ClO_4)_2(BDFDAAU)$ and (b) $CoCl_2$, $(NH_4)_6Mo_7O_{24}$, K_2PdCl_4, and $Hg(ClO_4)_2$.

these compounds in the cell growth of the different cell lines used; the same behaviour may be extended to the ligand BDFDAAU.

With the lower concentration of the Zn(II) complexes (2 μM), a significant increase was found in growth curves (Fig. 5). This positive effect can be explained because the zinc binds to cysteines in the DNA-binding domain of ER_α resulting in the formation of a protein motif referred to as a zinc finger which binds to an estrogen response element [34]. The replacement of zinc with other metals may alter the binding ability of the DNA-binding domain, so the testing of different complexes is very interesting from this point of view. At concentrations higher than 4 μM, the opposite effect is observed.

We can conclude these studies show up the ability of the compounds for acting as modulators of cell growth due to their estrogen-like characteristics. Thus, further studies are necessary to understand the mechanism involved in proliferation/antiproliferation induced by these compounds.

Acknowledgements

Thanks are due to Junta de Andalucía (FQM-273 PAIDI) for financial support.

References

[1] N.H. Pilkinton, R. Robson, Aust. J. Chem. 23 (1970) 2225–2236.
[2] H. Okawa, H. Furutachi, D.E. Fenton, Coord. Chem. Rev. 174 (1998) 51–75.
[3] A. Asokan, P.T. Manoharan, Inorg. Chem. 38 (1999) 5642–5654.
[4] S. Mohanta, S. Baitalik, S.K. Dutta, B. Adhikary, Polyhedron 16 (1998) 2669–2677.

[5] A.J. Atkints, D. Black, R.L. Finn, A. Marín-Becerra, A.J. Blake, L. Ruíz-Ramírez, W.S. Li, M. Schroder, Dalton Trans. (2003) 1730–1737.
[6] A. Erxleben, Inorg. Chem. 40 (2001) 412–414.
[7] U. Casellato, S. Tamburini, P. Tomasin, P.A. Vigato, S. Aime, M. Botta, Inorg. Chem. 38 (1999) 2906–2916.
[8] D. Black, A.J. Blake, K.P. Dancey, A. Harrison, M. McPartlin, S. Parsons, P.A. Tasker, G. Whittaker, M. Schröder, J. Chem. Soc. Dalton Trans. (1998) 3953–3960.
[9] S. Kita, H. Furutachi, H. Okawa, Inorg. Chem. 38 (1999) 4038–4045.
[10] H. Furutachi, A. Ishida, H. Miyasaka, N. Fukita, M. Ohba, H. Okawa, M. Koikawa, J. Chem. Soc. Dalton Trans. (1999) 367–372.
[11] J. Gradinaru, A. Forni, Y. Simonov, M. Popovici, S. Zecchin, M. Gdaniec, D.E. Fenton, Inorg. Chim. Acta 357 (2004) 2728–2736.
[12] B. Dutta, B. Adhikary, P. Bag, U. Florke, K. Nag, J. Chem. Soc. Dalton Trans. (2002) 2760–2767.
[13] P.A. Vigato, S. Tamburini, Coord. Chem. Rev. 248 (2004) 1717–2128.
[14] M. Paluch, J. Lisowski, T. Lis, Dalton Trans. (2006) 381–388.
[15] S. Khanra, T. Weyhermüller, E. Bill, P. Chaudhuri, Inorg. Chem. 45 (2006) 5911–5923.
[16] N. Sekine, T. Shiga, M. Ohba, H. Okawa, Bull. Chem. Soc. Jpn. 79 (2006) 881–885.
[17] S.M. Annigeri, A.D. Naik, U.B. Gandadharmath, V.K. Revankar, V.B. Mahale, Trans. Metal Chem. 27 (2002) 316–320.
[18] F. Hueso-Ureña, N.A. Illán-Cabeza, M.N. Moreno-Carretero, J.M. Martínez-Martos, M.J. Ramírez-Expósito, J. Inorg. Biochem. 94 (2003) 326–334.
[19] M. Tümer, N. Deligönül, A. Gölcü, E. Akgün, M. Dolaz, H. Demirelli, M. Digrak, Trans. Metal Chem. 31 (2006) 1–12.
[20] W.J. Geary, Coord. Chem. Rev. 7 (1971) 81–122.
[21] Hyperchem, release 6.0 for Windows, Molecular Modelling System. Hypercube, Inc. 2000.
[22] V. Ramesh, P. Umasundari, K.K. Das, Spectrochimica Acta A 54 (1998) 285–297.
[23] B. Humbert, M. Alnot, F. Quilès, Spectrochimica Acta A 54 (1998) 465–476.
[24] F. Hueso-Ureña, M.N. Moreno-Carretero, A.L. Peñas-Chamorro, J.M. Amigó, V. Esteve, T. Debaerdemaeker, Polyhedron 18 (1999) 3629–3636.
[25] D. Lin-Vien, N.B. Colthup, W.G. Fateley, J.G. Grasselli, The Handbook of Infrared and Raman Characteristic Frequencies of Organic Molecules, Academic Press, 1991.
[26] K. Nakamoto, Infrared and Raman Spectra of Inorganic and Coordination Compounds, fifth ed., Wiley & Sons, 1997.
[27] J.F. Ferraro, Low-Frequency Vibrations of Inorganic and Coordination compounds, Plenum Press, 1971.
[28] A.B.P. Lever, Inorganic Electronic Spectroscopy, second ed., Elsevier, 1984.
[29] K. Burger, Coordination Chemistry: Experimental Methods, Butterworth, 1973.
[30] B.J. Hathaway, Comprehensive coordination chemistry, in: G. Wilkinson, R.D. Gillard, J.A. McCleverty (Eds.), The Synthesis, Reactions, Properties and Applications of Coordination Compounds, vol. 5, Pergamon Press, Oxford, 1987, Section 53.
[31] R.L. Carlin, Magnetochemistry, Springer-Verlag, Berlin, 1986.
[32] B.J. Hathaway, E.D. Billing, Coord. Chem. Rev. 5 (1970) 143.
[33] N.A. Illán-Cabeza, A.R. García-García, M.N. Moreno-Carretero, J.M. Martínez-Martos, M.J. Ramírez-Expósito, J. Inorg. Biochem. 99 (2005) 1637–1645.
[34] M.B. Martin, R. Reiter, T. Pham, Y.R. Avellanet, J. Camara, M. Lahm, E. Pentecost, K. Pratap, B.A. Gilmore, S. Divekar, R.S. Dagata, J.L. Bull, A. Stoica, Endocrinology 144 (2003) 2425–2436.
[35] S. Safe, Nat. Med. 9 (2003) 1000–1001.
[36] S.Y. Choe, S.J. Kim, H.G. Kim, J.H. Lee, Y. Choi, H. Lee, Y. Kim, Sci. Total Environ. 312 (2003) 15–21.